This is an open access article published under an ACS AuthorChoice License, which permits copying and redistribution of the article or any adaptations for non-commercial purposes.

Macromolecules

Article

pubs.acs.org/Macromolecules

Termination Kinetics of Surface-Initiated Radical Polymerization Measured by Time-Resolved ESR Spectroscopy after Laser-Pulse Initiation

Julia Moehrke and Philipp Vana*

Institut für Physikalische Chemie, Georg-August-Universität Göttingen, Tammannstraße 6, D-37077 Göttingen, Germany

Supporting Information

ABSTRACT: The single-pulse−pulsed-laser polymerization−electron spin resonance (SP-PLP-ESR) method was used to study the termination reaction in polymerization of *n*-butyl methacrylate (*n*-BMA) from silica nanoparticles. The polymerization from the surface was initiated by the surface-attached photoinitiator 2,2-dimethoxy-2-phenyl-1-(2-(2-(trimethoxysilyl)ethyl)phenyl)ethane-1-one (DMPTS). The obtained termination rate coefficient at 335 K of k_t = (5.4 ± 0.7) × 10^6 L mol^{-1} s^{-1}, which could unambiguously be assigned to the termination reaction between two surface-attached macroradicals, is about 2 orders of magnitude smaller than the value found in homogeneous *n*-BMA polymerization. Surprisingly, no chain-length dependence of the termination rate coefficient could be observed. This fact and temperature-dependent studies of k_t, which yield an activation energy that is in perfect agreement with the activation energy of propagation of *n*-BMA, indicate that the termination between surface-attached macroradicals proceeds under reaction diffusion control, as their translational diffusion is suppressed.

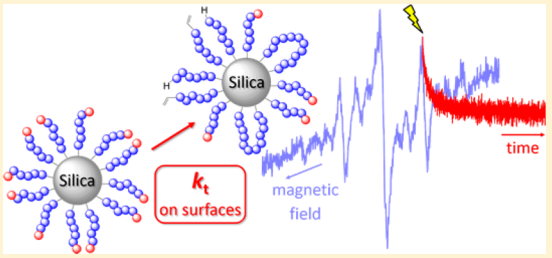

INTRODUCTION

Inorganic nanoparticles covered by covalently attached polymer chains have received increasing attention in recent years owing to their numerous applications in many scientific and medical fields, such as catalysis[1−4] and drug delivery systems.[5,6] Besides, imbedding of polymer-grafted nanoparticles as fillers into polymer matrices results in polymer nanocomposites with very promising material properties.[7−12] Even very small amounts of the filler material have an enormous impact on the material performance ascribed to the large specific surface area of nanoparticles. To allow a precise control of the nanocomposite's properties, a uniform dispersion of the inorganic particles in the polymer matrix is crucial. Without modifying the surface of the nanoparticles by polymer chains, they would agglomerate locally and segregate from the matrix because of their incompatibility with the polymer phase. By enhancing the compatibility between nanoparticles and the polymer matrix, the properties of the nanocomposites can be tuned and enhanced. For achieving this goal, the grafting-to and grafting-from methods are used to attach polymer chains covalently to surfaces.[13] While only small grafting densities and thin polymer films can be achieved by the grafting-to approach,[14−16] surface-initiated polymerizations lead to a better control of the grafting density and the layer thickness of the polymer. For the latter, surface-initiated radical polymerization, also including controlled polymerization methods,[17,18] has been especially successful.[13−15,19]

Knowing the exact kinetic behavior of surface-initiated polymerizations allows for the prediction of properties, e.g., the molar mass distribution of the grafted polymer chains, and is thus mandatory for directed material design. However, up to now, relatively little is known about the kinetic parameters of radical polymerizations from surfaces. In 1998, Prucker and Rühe performed the first investigations concerning the kinetics and mechanism of surface-initiated polymerizations of styrene from silica gel.[19] They concluded that the termination is heavily influenced when initiating the polymerization from surfaces instead of in solution, but no quantitative information has been given. Recently, we applied the pulsed-laser polymerization−size-exclusion chromatography (PLP-SEC) method in order to obtain information about the propagation kinetics of surface-tethered macroradicals.[20] We found that the propagation rate coefficient, k_p, of surface-bound radicals is slightly enhanced in comparison to free macroradicals, which may be indication of the fact that that the growing chains are not able to shield the active center as well as the macroradicals in solution, due to their surface anchorage.

In the present work, the termination kinetics of surface-tethered macroradicals is studied with state-of-the art measurement methods for the first time. For the determination of termination rate coefficients, k_t, in radical polymerization, the single-pulse−pulsed-laser polymerization−electron spin resonance (SP-PLP-ESR) technique has been verified to be a powerful tool. The SP-PLP-ESR technique—which rests on the time-resolved online tracing of macroradical concentration decay via ESR after single-pulse initiation—has already been

Received: March 30, 2015
Revised: April 30, 2015
Published: May 8, 2015

 © 2015 American Chemical Society

DOI: 10.1021/acs.macromol.5b00662
Macromolecules 2015, 48, 3190−3196

Scheme 1. Decomposition of the Surface-Attached Photoinitiator Silica−DMPTS

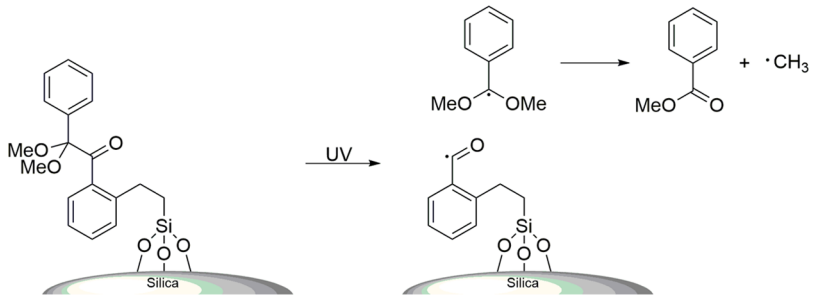

applied to many different homogeneous radical polymerization systems including polymerizations of numerous monomers in bulk, at different temperatures, and in several solvents.[21−24] However, the termination of radical polymerizations from nanoparticle surfaces has not been investigated by this method so far due to the demanding experimental setup.

The present work describes the first successful application of the SP-PLP-ESR technique for investigating the termination kinetics of surface-tethered macroradicals. For this explorative study we chose *n*-butyl methacrylate (*n*-BMA) as monomer and silica as the solid support. The latter was selected due to its unrivaled availability, chemical resistance, mechanical stability, transparency for the here applied UV radiation, and its numerous applications.[25] The silica nanoparticles were surface-functionalized by 2,2-dimethoxy-2-phenyl-1-(2-(2-(trimethoxysilyl)ethyl)phenyl)ethan-1-one (DMPTS), which allows photoinitiation at the surface. The decomposition behavior of this surface-attached initiator was investigated by thermogravimetric analysis (TGA) and soft ionization mass spectrometry.

EXPERIMENTAL SECTION

Materials. The monomer *n*-BMA (Aldrich, 99%, stabilized with 10 ppm monomethyl ether hydroquinone) was passed through a column filled with inhibitor remover (Aldrich). The silica nanoparticles (Aldrich) had an average diameter of 12 nm and a specific surface area of 175−225 m^2/g according to the manufacturer. All other chemicals were obtained commercially and used without further purification.

Synthesis of 2,2-Dimethoxy-2-phenyl-1-(2-(2-(trimethoxysilyl)ethyl)phenyl)ethane-1-one (DMPTS). DMPTS was synthesized following a procedure reported in ref 26. To a mixture of 2,2-dimethoxy-2-phenylacetophenon (DMPA) (2.59 g, 10.1 mmol, 1.0 equiv), dichloro(*p*-cymene)ruthenium(II) dimer (164 mg, 268 μmol, 2.7 mol %), triphenylphosphine (401 mg, 1.53 mmol, 15 mol %), and sodium formate (274 mg, 4.03 mmol, 40 mol %) in toluene (anhydrous, 10 mL), trimethoxy(vinyl)silane (3.01 g, 20.3 mmol, 2.0 equiv) was added. The reaction mixture was stirred, degassed via argon-bubbling, and heated to reflux for 2 days. The solvent was removed under reduced pressure, and the crude mixture was purified by silica gel chromatography (ethyl acetate/cyclohexane 4:21 → 3:7). The target compound (1.55 g, 3.83 mmol, 38%) was obtained as a yellow oil. ^{1}H NMR (300 MHz, $CDCl_3$) δ (ppm) = 0.87−0.96 (m, 2 H, Si−CH_2), 2.46−2.54 (m, 2 H, Si−CH$_2$−CH_2), 3.29 (s, 6 H, C(O−CH_3)$_2$), 3.53 (s, 9 H, Si(O−CH_3)$_3$), 7.04−7.12 (m, 1 H, Ar−*H*), 7.17−7.22 (m, 1 H, Ar−*H*), 7.27−7.37 (m, 4 H, 4 × Ar−*H*), 7.48−7.54 (m, 1 H, Ar−*H*), 7.57−7.62 (m, 1 H, Ar−*H*). MS (ESI, positive mode, *m*/*z*): found: 427.2; calculated: 427.2 ([M + Na]$^+$).

Immobilization of DMPTS on Silica Nanoparticles. To silica nanoparticles (1.03 g), a solution of DMPTS (600 mg, 1.48 mmol) in toluene (anhydrous, 30 mL) was added. The suspension was degassed and stirred for 2 days under reflux. The particles were purified by three cycles of isolation by centrifugation and redispersion in acetone.

Polymerization Procedure. To DMPTS-functionalized silica nanoparticles (110 mg), a solution of *n*-BMA (60.0 mg, 0.42 mmol) in benzene (5 mL) was added. The sample was degassed via argon-bubbling and polymerized for 20 h at room temperature. For continuous photoinitiation, an N-8 UV lamp (Benda Konrad) with an emission wavelength of 366 nm was used.

Thermogravimetric Analysis (TGA). TGA was conducted with a Netzsch TG 209 F3 Tarsus from room temperature up to 1000 °C with a heating rate of 10 K/min under a nitrogen atmosphere with a flow rate of 20 mL/min.

Mass Spectrometry. Mass spectra of polymer samples were recorded with an electrospray-ionization (ESI) maXis mass spectrometer (Bruker Daltonics Inc.). The measuring range was between 300 and 2900 *m*/*z* with a spray voltage of 3800 V and a capillary temperature of 180 °C. The inert gas flow was 4 L min^{-1} with a pressure of 0.3 bar. The samples were measured in a mixture of tetrahydrofuran and methanol with formic acid being the additive.

Time-Resolved ESR (TR-ESR) Measurements. The TR-ESR spectra were recorded on a Bruker ESR CW/transient spectrometer system Elexsys-II 500T with an ER 41122SHQE-LC cavity (Bruker). The ESR sample tubes were fitted into the cavity equipped with a grid allowing irradiation of the sample by a XeF laser (LPX 210 iCC, Lamda Physik) with a wavelength of 351 nm and a pulse energy of about 50 mJ/pulse. A Quantum Composers 9314 pulse generator (Scientific Instruments) synchronized the ESR spectrometer and the laser source. Temperature control in the range from 295 to 335 K was achieved via an ER 4131VT unit (Bruker) by purging the cavity with nitrogen.

Samples were prepared according to the following procedure: To DMPTS-functionalized silica nanoparticles (56 mg), *n*-BMA (*c*(BMA) = 3.1 mol L^{-1}) and benzene (2 mL) were added. The mixture was stirred overnight under exclusion of visible light to achieve a good dispersion of the nanoparticles. After that, oxygen was removed by several freeze−pump−thaw cycles. In a glovebox 0.15 mL of the sample mixture was filled into each ESR tube. The tubes were sealed with plastic caps, and Parafilm and used immediately after preparation.

Prior to SP-PLP-ESR measurements, an ESR spectrum was recorded under pseudostationary PLP conditions with a laser repetition rate of 20 Hz to identify the peak maximum positions for TR-ESR experiments. Previously, experimental parameters, in particular, the modulation amplitude and the microwave energy, were adjusted. For obtaining absolute radical concentrations, a calibration with (2,2,6,6-tetramethylpiperidin-1-yl)oxidanyl (TEMPO, 98%; Aldrich) was done following a procedure described elsewhere.[22]

RESULTS AND DISCUSSION

Initiator. DMPA is a common commercially available photoinitiator and can be functionalized in a ruthenium-catalyzed reaction that allows the regioselective alkylation of aromatic ketones at the ortho position of the keto substituent using vinylsilanes,[26] resulting in the photoinitiator DMPTS (see Scheme 1, left). In this work, DMPTS was covalently attached to silica nanoparticles in an immobilization reaction for the first time. The immobilization reaction was conducted in anhydrous

DOI: 10.1021/acs.macromol.5b00662
Macromolecules 2015, 48, 3190−3196

toluene under reflux for direct condensation of the surface silanol groups and the silane group of the initiator resulting in stable siloxy bonds. The successful immobilization of DMPTS onto silica nanoparticles was proven by TGA (see Figure S1 of the Supporting Information) with the result of a grafting density of about 0.9 molecules of DMPTS per nm^2.

Using photoinitiated polymerizations of *n*-BMA in solution of benzene (which was used to minimize chain transfer, whereby the radicals could leave the surface), the photodecomposition behavior of the surface-attached DMPTS was investigated in more detail. The amount of polymer formed by this solid-supported initiator was found by TGA to be 40 wt % of the obtained dry material consisting of particles and polymer (see Figure S2 of the Supporting Information). After washing several times with tetrahydrofuran and drying the sample again, the amount of polymer decreased to 37%, indicating that a small amount of nonanchored polymer was formed during the process in addition to the large majority of surface-attached polymer. DMPA-type photoinitiators have been studied extensively concerning its photodecomposition behavior.[27−29] According to literature, it is anticipated that the photolysis of silica-grafted DMPTS results in a benzoyl-type radical covalently attached to the surface and a nonanchored dimethoxybenzyl radical that can undergo a secondary fragmentation giving methyl benzoate and a methyl radical (see Scheme 1). The dimethoxybenzyl radical is known to initiate the polymerization to a much smaller extent than benzoyl-type radicals do.[30,31] In addition, methyl radicals have been postulated to act predominantly as terminating moieties due to their high reactivity and diffusivity.[30] This is in agreement with the results from the TGA measurements, indicating that most of the poly(*n*-BMA) formed by silica-grafted DMPTS is indeed grafted to the particle surface. However, the rate of the secondary fragmentation reaction of the dimethoxybenzyl radical (see Scheme 1), which may influence the amount of nongrafted polymer formed, is known to depend on polymerization conditions, more precisely light intensity and temperature.[32] Thus, it is of value to examine the end groups of nongrafted polymer by electrospray ionization−mass spectrometry (ESI-MS) measurements. In Figure S3 (see Supporting Information) the mass spectrum of one complete repeat mass unit of poly(*n*-BMA) is highlighted. Possible combination and disproportionation products formed in solution, initiated by the nonanchored methyl and dimethoxybenzyl radicals, are illustrated in Table S1 (see Supporting Information). The mass spectrum shows that methyl radicals mainly initiate the polymerization in solution under this condition. The ratio of disproportionation products of methyl-initiated polymers to the ones of dimethoxybenzyl-initiated polymers is approximately 6.4:1, indicating that under given polymerization conditions the fragmentation of the acetal fragment is faster than the initiation by this radical. The quantity of disproportionation products being almost equal to the one of combination products suggests that none of these two termination mechanisms is favored, which is in line with recent studies from our lab.[33]

ESR Spectroscopy Experiments. At first, the decomposition behavior of the silica-grafted DMPTS in solution of benzene (without monomer) was investigated by ESR measurements. Figure 1a (black line) shows the corresponding ESR spectrum recorded under continuous pulsed-laser initiation at a pulse repetition rate of 20 Hz. The spectrum results from an overlay of spectra of three different radical species: (i) the surface-attached benzoyl-type radical, (ii) the free dimethoxybenzyl radical, and (iii) the free methyl radical. It is anticipated that the radicals that are not anchored to the silica particle surface terminate quickly with each other or with the surface-grafted initiator fragments, since they swiftly diffuse through the liquid media, while the termination of two benzoyl-type radicals is dramatically slowed down, due to their fixed position on the silica particles which hinder translational diffusion. The arrows in Figure 1a mark peaks of the ESR spectrum obtained under continuous pulsed-laser initiation (black line) that disappeared completely 35 s after the irradiation has stopped (see Figure 1a, red line), indicating

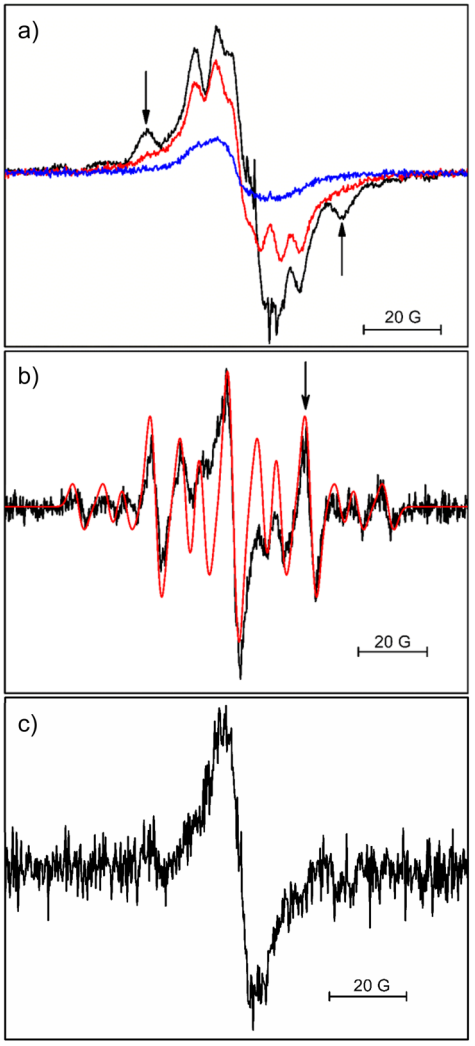

Figure 1. (a) ESR spectrum of silica−DMPTS in benzene under continuous pulsed-laser initiation measured at a repetition rate of 20 Hz at 335 K. The red and blue lines illustrate the ESR spectra recorded 35 s and 16 min after irradiation, respectively. (b) ESR spectrum of *n*-BMA polymerization in benzene ($c(n\text{-BMA}) = 3.1$ mol L^{-1}) under pseudostationary PLP conditions measured at a repetition rate of 20 Hz at 295 K with silica−DMPTS being the photoinitiator. The red line represents the simulated poly(*n*-BMA) radical spectrum fitted with hyperfine coupling constants of $a(\beta\text{-H}_1) = 14.0$ G, $a(\beta\text{-H}_2) = 8.8$ G, and $a(\text{CH}_3) = 22.5$ G.[34] (c) ESR spectrum corresponding to the long-living surface-attached benzoyl-type radicals during the polymerization of *n*-BMA in benzene ($c(n\text{-BMA}) = 3.1$ mol L^{-1}) with silica−DMPTS being the initiator recorded 1.5 min after irradiation at 295 K. The spectra were recorded at a modulation amplitude of 3 G, a sweep time of 5.24 s, and an attenuation of 25 dB.

DOI: 10.1021/acs.macromol.5b00662
Macromolecules 2015, 48, 3190−3196

that there are radicals that terminate readily, as expected. Another ESR spectrum was recorded 16 min after the irradiation has stopped (see Figure 1a, blue line). The obtained broad singlet in the ESR spectrum corresponds to the above-mentioned long-lived benzoyl-type radicals that are attached to the silica particles and that are missing termination partners in their neighborhood.

Then, monomer was added. Figure 1b (black line) shows the ESR spectrum recorded during PLP of *n*-BMA in benzene with silica−DMPTS being the photoinitiator. It is in good qualitative agreement with the simulated 13-line ESR spectrum (Figure 1b, red line) for methacrylate polymerizations with $a(\beta\text{-H}_1)$ = 14.0 G, $a(\beta\text{-H}_2)$ = 8.8 G, and $a(\text{CH}_3)$ = 22.5 G[34] being the coupling constants. However, deviations between the two spectra can be observed especially in the center of the shown field regime, indicating that the measured spectrum is an overlay of the spectrum of the propagating radical during *n*-BMA polymerization and the spectrum of another radical species, probably resulting from an initiator fragment. This radical species must be relatively stable. Otherwise, it would initiate the *n*-BMA polymerization rapidly as well, transforming itself into a poly(*n*-BMA) macroradical, and would thus not show up as an individual species. Prucker and Rühe[19] suggested that during the thermally initiated polymerization of styrene from silica nanoparticles a big portion of surface-attached initiator radicals does not initiate the polymerization because of a cage effect. In a theoretical study, Xue et al.[35] showed that this effect increases with increasing grafting density of the initiator and decreasing surface curvature. In our work, high grafting densities of the initiator were intended because relatively high radical concentrations are beneficial for the ESR experiments. It is thus very likely that the second radical species observed in the ESR spectrum during *n*-BMA polymerization is the benzoyl-type surface-attached radical that is shielded by grafted polymer chains and/or other surface-attached molecules. To investigate this phenomenon in more detail, several ESR spectra were recorded and analyzed after specific time intervals after the irradiation of the sample has stopped. Figure 1c illustrates the spectrum obtained 1.5 min after PLP. As expected, the signal has a shape similar to the ESR spectrum that was attributed to the benzoyl-type surface-attached radical species (Figure 1a, blue line).

The time evolution of the benzoyl-type radical concentration is shown in Figure 2. The concentration decreases very slowly because of the limited accessibility of the surface-attached initiator-derived radicals for other radicals. It can only be speculated how the termination of these surface-bound radicals occur, but the most likely mechanism occurs via the slow transfer to a solution molecule, whereby the radical is released from the surface and can then readily terminate. These processes will be subject of forthcoming studies.

In order to exclude the influence of this relatively stable radical on the investigations of the termination reaction of the growing chains in *n*-BMA polymerization from silica particles, a fixed magnetic field position was chosen for the time-resolved SP-PLP-ESR measurements, which exclusively corresponds to the growing macroradical (marked by an arrow in Figure 1b). This peak is not overlapping with signals from the stable benzoyl-type radical, as evident from the excellent match with the simulated spectrum. Figure 3 illustrates the measured macroradical concentration vs time curve after applying a single laser pulse at 335 K. Please note that the portion of surface-attached, stable benzoyl radicals is masked in this experiment.

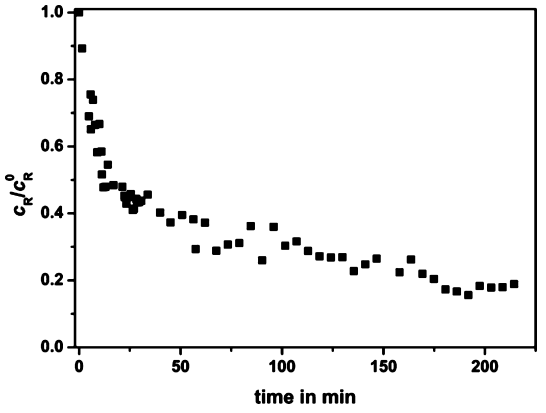

Figure 2. Normalized radical concentration vs time trace for the long-living benzoyl-type radical species during the polymerization of *n*-BMA in benzene with silica−DMPTS being the initiator. Data points were determined by measuring the double integral of the ESR signal at different times after irradiation of the sample and application of a radical concentration calibration.

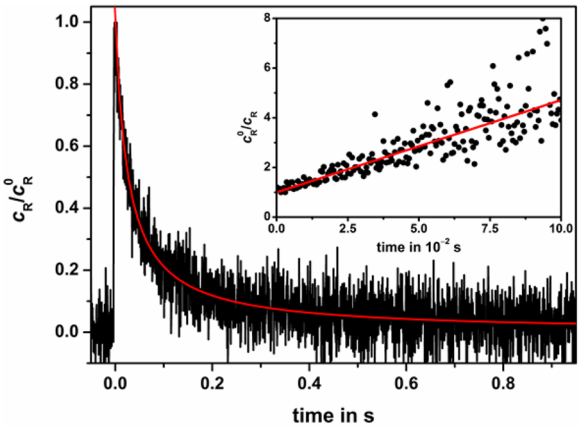

Figure 3. Normalized ESR intensity vs time trace for *n*-BMA polymerization in benzene (c(*n*-BMA) = 3.1 mol L^{-1}) at 335 K with silica−DMPTS being the photoinitiator. About 110 individual traces were coadded to obtain the SP-PLP-ESR signal. ESR intensity was measured at the magnetic field position indicated in Figure 1b. The initial radical concentration was close to 3.4×10^{-6} mol L^{-1}. The red line represents a fit of the experimental ESR-derived data to eq 2. The inset illustrates the reciprocal radical concentration vs time. The straight red line is the linear fit that intersects the ordinate at $c_R^0/c_R = 1$. The analysis in the inset is restricted to the time region $t \leq 0.1$ s because of diminishing signal quality.

Assuming ideal second-order termination kinetics (i.e., k_t assuming as being constant throughout the process), eq 1 holds

$$-\frac{dc_R}{dt} = 2k_t {c_R}^2 \quad (1)$$

with k_t being the termination rate coefficient for the termination of two macroradicals and c_R being the macroradical concentration.

The signal-to-noise quality of the obtained SP-PLP-ESR data is not sufficient for high-resolution first-derivative curves, as would be required for fitting eq 1 directly. Thus, the integrated expression (eq 2) derived from eq 1

$$\frac{c_R}{c_R^0} = \frac{1}{1 + 2k_t c_R^0 t} \quad (2)$$

DOI: 10.1021/acs.macromol.5b00662
Macromolecules 2015, 48, 3190−3196

with c_R^0 being the macroradical concentration at time $t = 0$ was fitted to the experimental data (Figure 3, red line). According to eq 2, k_t can be determined from the slope of a plot of the reciprocal radical concentration vs time. In the ideal case that k_t is chain length independent, such a plot yields a straight line that intersects the ordinate at $c_R^0/c_R = 1$. If chain length dependence of k_t would be operational, this simple second-order kinetics would not hold anymore, and the interpretation of the experimental data would become more complicated, as demonstrated by Buback et al.[24] The inset in Figure 3 illustrates that a linear fit according to the reciprocal of eq 2 of the experimental data is extremely satisfactory, indicating that k_t in this experiment is *chain length independent*. This finding is truly surprising and in contrast to the generally accepted concept of a chain length dependent k_t for homogeneous radical polymerization systems.[36,37] The evaluated value of $k_t = (5.4 \pm 0.7) \times 10^6$ L mol^{-1} s^{-1} for the here investigated surface-attached macroradicals is under the given conditions about *2 orders of magnitude smaller* than the literature value obtained for the termination of two radicals of chain length one ($k_t^{1,1} = 3.0 \times 10^8$ L mol^{-1} s^{-1} [22]) in homogeneous *n*-BMA polymerization, which was obtained via extrapolation of experimental k_t values at different chain lengths to chain length one.

The smaller value of k_t can easily be understood by a reduced mobility of the radical centers due to the covalent attachment of the macroradicals to the surface. A closer look to the mechanism of this special case of termination will be presented below. The fact, however, that a slower k_t is observed in this system allows for a first important conclusion: The system is designed in such a way that initiator-derived radicals are formed both upon the surface and also in solution (see Scheme 1). Free radicals in solution, as indicated by the ESI-MS experiments presented above, also initiate BMA polymerization to some extent. The corresponding free macroradicals in homogeneous solution phase, however, are known to terminate quickly ($k_t^{1,1} = 3.0 \times 10^8$ L mol^{-1} s^{-1} [22]) and will thus not be observable on the time scale presented in Figure 3. When they terminate in solution, they leave behind surface-attached radicals due to the stoichiometry of the initiator decomposition. A small portion of termination between free radicals and surface attached radicals (cross-termination) may also occur, which is expected to be possibly a little smaller than the homogeneous phase k_t, but there are not enough radicals in solution left—due to their swift homotermination—to terminate all the surface-attached radicals. As a consequence, surface-attached radicals will eventually "be alone" in the system after a short period of time after the laser pulse, in which the homotermination and cross-termination of the free macroradicals in solution occur. The relatively slow termination activity being observable on the long time scale, as indicated in Figure 3, can thus unambiguously be assigned to the termination between two surface-attached macroradicals.

The question needs to be answered now as to why this termination between surface-attached radicals is not chain length dependent. Two reasons may be hypothesized:

(1). Segmental Diffusion May Dominate over the Entire Chain-Length Regime. For classical, homogeneous polymerization systems, the chain length dependence of k_t is explained by decreasing diffusion with increasing chain length.[36] Two different chain length regimes are common: First, k_t of homogeneous polymerization systems decrease rapidly under center-of-mass diffusion control assuming that chain entanglements play no major role. Above a critical crossover chain length, i_c, the termination reaction in homogeneous systems is controlled by segmental diffusion of two entangled chains, resulting in a much weaker chain length dependency with exponents in the respective power law of 0.1 and below, depending on the system.[38,39] The overall situation clearly changes when termination of surface-initiated macroradicals is considered, as the growing chains are fixed to the surface with one terminal end resulting in decreased translational diffusion and changed local polymer segment densities at the reaction site. With an increasing number of pulses (the radical concentration vs time trace illustrated in Figure 3 is averaged from about 110 individual single-pulse measurements in order to achieve a good signal-to-noise quality), the surface coverage of particles with polymer increases. This surface-bound polymer influences the growing chains because of the spatial proximity, which is in contrast to the polymerization in solution, where growing polymer chains can move nearly independently from dead polymer. This might be a reason why short growing chains on the surface behave similarly to long ones in solution when considering the termination reaction. The short chains on the surface may also experience high polymer segment densities around themselves, which leads to segmental diffusion control that shows only a very small chain length dependency, which may be too small to be seen pronouncedly.

(2). Reaction Diffusion May Dominate. Alternatively, one may speculate that the termination between surface-bound macroradicals is occurring under reaction diffusion control;[40] i.e., the approximation of radical centers toward each other only proceeds via propagation, whereby the position of the radical chain end changes, instead of diffusive molecular movements of the entire chain. The latter are clearly reduced—if not disabled at all—by the covalent attachment. Reaction diffusion is mainly considered as being chain length independent, as the propagation rate is (nearly) not depending on chain length. Specific chain length dependencies of k_p only relate to the very first propagation steps[41] or are very small,[42] so that they are not of importance here.

In order to decide which of the two hypotheses may be correct, we evaluated the activation energy of the termination reaction of surface-bound macroradicals. If segmental diffusion over the entire chain- length regime would be the cause of the not observable chain length dependency, one would expect an activation energy of k_t that is similar to the already known literature data of $E_A(k_t,n\text{-BMA}) = 9.9$ kJ mol^{-1},[43] reflecting the temperature dependence of monomer fluidity. If reaction diffusion would be operational, one would expect an activation energy that reflects the temperature dependency of k_p of *n*-BMA polymerization, which has been reported to be $E_A(k_p,n\text{-BMA}) = 22.9$ kJ mol^{-1}.[44]

Figure 4 shows the temperature dependence of the k_t values of the surface-initiated polymerization of *n*-BMA as an Arrhenius plot. The data can best be fitted by the following linear function eq 3

$$\ln k_t = 23.9 - 2682\left(\frac{T^{-1}}{\mathrm{K}^{-1}}\right) \tag{3}$$

leading to an experimental activation energy of $E_A(k_t) = 22.3 \pm 7.0$ kJ mol^{-1}. This value is in excellent agreement with the activation energy of k_p (22.9 kJ mol^{-1}) and clearly supports the second hypothesis, i.e., that reaction diffusion is operational.

The last question that needs to be addressed before a complete and comprehensive picture emerges is why the

DOI: 10.1021/acs.macromol.5b00662
Macromolecules 2015, 48, 3190−3196

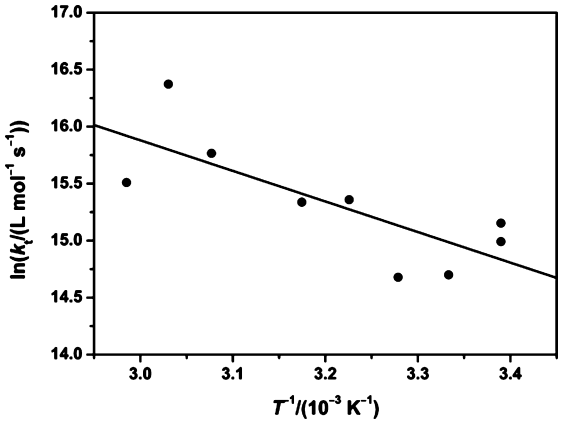

Figure 4. Arrhenius plot of the termination rate coefficient of the surface-initiated polymerization of *n*-BMA in benzene (c(*n*-BMA) = 3.1 mol L^{-1}) with silica−DMPTS being the surface-attached initiator.

experimental k_t value found in this work—although being significantly reduced in comparison to the homogeneous phase value—still is relatively high for a reaction diffusion-controlled k_t. Homogeneous k_t values of methyl methacrylate in the reaction diffusion control regime were found to be around 10^4 L mol^{-1} s^{-1},[40] which is 2 orders of magnitude lower than the values found in the present study. Two reasons may be responsible for this: (i) First, the situation in the homogeneous phase reaction control regime, where chains are truly locked in a polymer matrix and cannot move at all, is different from the scenario being operational in the present surface-confined system, where the chains still have some flexibility to move around, although they are hindered from overall translational diffusion. This remaining freedom of macromolecular motion may increase the k_t value. (ii) One should be aware of the fact that all the kinetic treatments performed in this study are relying on rate laws, in which reaction rates are correlated with species concentrations, as is common in kinetics. The species concentration, however, is assumed to be homogeneously distributed over the system, i.e., macroscopic and microscopic concentration values are considered as being identical. This is truly not the case for surface-confined initiator systems, where radicals are not evenly distributed all over the system but are only located on the surface of particles. The operational reaction volume is thus greatly reduced; the microscopic concentrations of radicals are thus much higher at the site of reaction in comparison to the macroscopic values that were calculated by the overall volume. Higher actual concentrations of radicals would require lower actual k_t values in order to produce the same experimentally observed radical vs time traces. The true, actual k_t values may thus be indeed lower—as would be expected for reaction diffusion-controlled k_t—than the apparent, in this work calculated k_t values.

CONCLUSIONS

ESR studies of the termination reaction in polymerization of *n*-BMA from silica nanoparticles were successfully performed using the silica-immobilized photoinitiator DMPTS. SP-PLP-ESR investigations yielded a k_t value that is about 2 orders of magnitude smaller than the literature value of k_t in homogeneous *n*-BMA polymerization under similar conditions. In contrast to polymerizations in homogeneous phase, k_t for the polymerization from silica particles showed no chain length dependence. Temperature-dependent experiments yielded an activation energy of the termination process that is in harmony with the concept that the termination of the surface-attached macroradicals proceeds under reaction diffusion control, as their translational diffusion is suppressed. The results demonstrate that the termination kinetics of surface-initiated radical polymerizations can successfully be investigated by the SP-PLP-ESR method, opening up the way to more detailed studies of various inhomogeneous systems.

ASSOCIATED CONTENT

Supporting Information

Additional TGA diagrams; mass spectrometric analysis of polymer samples. The Supporting Information is available free of charge on the ACS Publications website at DOI: 10.1021/acs.macromol.5b00662.

AUTHOR INFORMATION

Corresponding Author

*E-mail pvana@uni-goettingen.de (P.V.).

Notes

The authors declare no competing financial interest.

DEDICATION

Dedicated to Prof. Michael Buback on the occasion of his 70th birthday.

REFERENCES

(1) Lu, Y.; Mei, Y.; Drechsler, M.; Ballauff, M. *Angew. Chem., Int. Ed.* **2006**, *45* (5), 813−816.
(2) Ballauff, M.; Lu, Y. *Polymer* **2007**, *48* (7), 1815−1823.
(3) Lu, Y.; Mei, Y.; Ballauff, M.; Drechsler, M. *J. Phys. Chem. B* **2006**, *110* (9), 3930−3937.
(4) Li, D.; Dunlap, J. R.; Zhao, B. *Langmuir* **2008**, *24* (11), 5911−5918.
(5) Ferrari, M. *Nat. Rev. Cancer* **2005**, *5* (3), 161−171.
(6) Peer, D.; Karp, J. M.; Hong, S.; Farokhzad, O. C.; Margalit, R.; Langer, R. *Nat. Nanotechnol.* **2007**, *2* (12), 751−760.
(7) Ash, B. J.; Siegel, R. W.; Schadler, L. S. *Macromolecules* **2004**, *37* (4), 1358−1369.
(8) Kumar, S. K.; Jouault, N.; Benicewicz, B.; Neely, T. *Macromolecules* **2013**, *46* (9), 3199−3214.
(9) Kumar, S. K.; Krishnamoorti, R. *Annu. Rev. Chem. Biomol. Eng.* **2010**, *1*, 37−58.
(10) Sanchez, C.; Julián, B.; Belleville, P.; Popall, M. *J. Mater. Chem.* **2005**, *15* (35−36), 3559−3592.
(11) Bansal, A.; Yang, H.; Li, C.; Cho, K.; Benicewicz, B. C.; Kumar, S. K.; Schadler, L. S. *Nat. Mater.* **2005**, *4* (9), 693−698.
(12) Bansal, A.; Yang, H.; Li, C.; Benicewicz, B. C.; Kumar, S. K.; Schadler, L. S. *J. Polym. Sci., Part B: Polym. Phys.* **2006**, *44* (20), 2944−2950.
(13) Tu, H.; Heitzman, C. E.; Braun, P. V. *Langmuir* **2004**, *20* (19), 8313−8320.
(14) Prucker, O.; Rühe, J. *Macromolecules* **1998**, *31* (3), 592−601.
(15) Biesalski, M.; Rühe, J. *Langmuir* **2000**, *16* (4), 1943−1950.
(16) Edmondson, S.; Osborne, V. L.; Huck, W. T. S. *Chem. Soc. Rev.* **2004**, *33* (1), 14−22.
(17) Huebner, D.; Koch, V.; Ebeling, B.; Mechau, J.; Steinhoff, J. E.; Vana, P. *J. Polym. Sci., Part A: Polym. Chem.* **2015**, *53* (1), 103−113.
(18) Rotzoll, R.; Vana, P. *J. Polym. Sci., Part A: Polym. Chem.* **2008**, *46* (23), 7656−7666.
(19) Prucker, O.; Rühe, J. *Macromolecules* **1998**, *31* (3), 602−613.
(20) Rotzoll, R.; Vana, P. *Macromol. Rapid Commun.* **2009**, *30* (23), 1989−1994.
(21) Kattner, H.; Buback, M. *Macromol. Chem. Phys.* **2014**, *215* (12), 1180−1191.

DOI: 10.1021/acs.macromol.5b00662
Macromolecules 2015, 48, 3190−3196

(22) Barth, J.; Buback, M.; Hesse, P.; Sergeeva, T. *Macromolecules* **2009**, *42* (2), 481−488.
(23) Barth, J.; Buback, M. *Macromol. Rapid Commun.* **2009**, *30* (21), 1805−1811.
(24) Buback, M.; Egorov, M.; Junkers, T.; Panchenko, E. *Macromol. Rapid Commun.* **2004**, *25* (10), 1004−1009.
(25) Radhakrishnan, B.; Ranjan, R.; Brittain, W. J. *Soft Matter* **2006**, *2* (5), 386−396.
(26) Martinez, R.; Simon, M.-O.; Chevalier, R.; Pautigny, C.; Genet, J.-P.; Darses, S. *J. Am. Chem. Soc.* **2009**, *131* (22), 7887−7895.
(27) Fischer, H.; Baer, R.; Hany, R.; Verhoolen, I.; Walbiner, M. *J. Chem. Soc., Perkin Trans. 2* **1990**, 787−798.
(28) Faria, J. L.; Steenken, S. *J. Chem. Soc., Perkin Trans. 2* **1997**, 1153−1159.
(29) Fouassier, J.-P.; Merlin, A. *J. Photochem.* **1980**, *12* (1), 17−23.
(30) Szablan, Z.; Lovestead, T. M.; Davis, T. P.; Stenzel, M. H.; Barner-Kowollik, C. *Macromolecules* **2007**, *40* (1), 26−39.
(31) Barner-Kowollik, C.; Vana, P.; Davis, T. P. *J. Polym. Sci., Part A: Polym. Chem.* **2002**, *40* (5), 675−681.
(32) Gruber, H. F. *Prog. Polym. Sci.* **1992**, *17* (6), 953−1044.
(33) Buback, M.; Günzler, F.; Russell, G. T.; Vana, P. *Macromolecules* **2009**, *42* (3), 652−662.
(34) Hermosilla, L.; Sieiro, C.; Calle, P.; Zerbetto, M.; Polimeno, A. *J. Phys. Chem. B* **2008**, *112* (36), 11202−11208.
(35) Xue, Y.-H.; Zhu, Y.-L.; Quan, W.; Qu, F.-H.; Han, C.; Fan, J.-T.; Liu, H. *Phys. Chem. Chem. Phys.* **2013**, *15* (37), 15356−15364.
(36) Buback, M.; Egorov, M.; Gilbert, R. G.; Kaminsky, V.; Olaj, O. F.; Russell, G. T.; Vana, P.; Zifferer, G. *Macromol. Chem. Phys.* **2002**, *203* (18), 2570−2582.
(37) Barner-Kowollik, C.; Buback, M.; Egorov, M.; Fukuda, T.; Goto, A.; Olaj, O. F.; Russell, G. T.; Vana, P.; Yamada, B.; Zetterlund, P. B. *Prog. Polym. Sci.* **2005**, *30* (6), 605−643.
(38) Smith, G. B.; Russell, G. T.; Heuts, J. P. A. *Macromol. Theory Simul.* **2003**, *12* (5), 299−314.
(39) Olaj, O. F.; Zoder, M.; Vana, P. *Macromolecules* **2001**, *34* (3), 441−446.
(40) Buback, M. *Makromol. Chem.* **1990**, *191* (7), 1575−1587.
(41) Gridnev, A. A.; Ittel, S. D. *Macromolecules* **1996**, *29* (18), 5864−5874.
(42) Olaj, O. F.; Vana, P.; Zoder, M.; Kornherr, A.; Zifferer, G. *Macromol. Rapid Commun.* **2000**, *21* (13), 913−920.
(43) Buback, M.; Junkers, T. *Macromol. Chem. Phys.* **2006**, *207* (18), 1640−1650.
(44) Vana, P.; Barner-Kowollik, C.; Davis, T. P.; Matyjaszewski, K. In *Encyclopedia of Polymer Science and Technology*; Mark, H. F., Ed.; Wiley-Interscience: Hoboken, NJ, 2004; pp 359−472.

DOI: 10.1021/acs.macromol.5b00662
Macromolecules 2015, 48, 3190−3196